BUREAU INTERNATIONAL DES POIDS ET MESURES

Calculation of the effective area of DHI piston-cylinder No. 517,
working in the absolute mode at a nominal pressure of 1000 hPa

Richard Davis
BIPM

November 2006

Pavillon de Breteuil, F-92312 SEVRES cedex

Calculation of the effective area of DHI piston-cylinder No. 517, working in the absolute mode at a nominal pressure of 1000 hPa

Richard Davis
Bureau International des Poids et Mesures, 92312 Sèvres Cedex, France

Introduction:

The BIPM is now basing its pressure calibrations on a DH Instruments pressure balance (Model PG7607) operating in the absolute mode. The piston-cylinder of this balance has a nominal diameter of 50 mm so that it is possible to calculate the effective area, A, at 20 °C based on dimensional measurements taken at that reference temperature. In our case, the diameters at several locations along the axis of both the piston and cylinder were calibrated by the Laboratoire National de Métrologie et d'Essais (LNE, France). In addition, the same laboratory kindly provided us with circularity measurements taken at several locations along the axis of the piston and the cylinder. References [1,2,3,4] describe the principles behind our calculation.

The calculations proceed in three steps:

1. Determination of A_0, the effective area of the piston-cylinder in the limit of negligible pressure gradient along the engagement length [1,4];

2. Determination of A_P to take account of gas flow in the absolute mode, when the measured pressure is near $P_0 = 1000$ hPa [1,2,3,4]; and

3. Uncertainty budget [2,3,4,7].

I. Determination of A_0

Our piston-cylinder is the type described by Dadson et al. [1] as "I(B) Simple, Inverted". The equations describing this design are identical to the more usual "I(A) Simple, Upright" provided one places the origin of the vertical axis (z-axis) at the *top* of the engagement length, the positive z-axis extending downward. We use the following parameters, all of which are defined in [1]:

r : radius of the piston along the engagement length

r_0 : $r(z=0)$

R : radius of the cylinder along the engagement length

R_0 : $R(z=0)$

L : piston-cylinder engagement length, nominally 40 mm

P : pressure along the engagement length

Additional parameters are defined from the above as

$u = r - r_0$

$U = R - R_0$

$h_0 = R_0 - r_0$, nominally 0.000 8 mm

$h = R - r$

The final report of EUROMET Project 740 [4] gives a number of equivalent equations that may be used to determine *A* in the limit $P(L) = P(0)$. A typical formula is that of the PTB, which is also given in [1] (Eq. 35):

$$A_0 = \pi r_0^2 \left\{ 1 + \frac{h_0}{r_0} + \frac{1}{r_0} \frac{\int_0^L \frac{(u+U)}{h^3} dz}{\int_0^L \frac{1}{h^3} dz} \right\} \tag{1}$$

This equation is easily transformed to the equation used by the LNE [4], where the only parameters that appear are r_0, r, R and the limit of integration (L).

Such equations are readily solved provided that the necessary functions of *z* can be written in analytical form as, for example, as a power series in *z*. Integrations were carried out numerically using the packaged software, Mathcad 13.

We have only a limited number of measured diameters, supplied by the LNE, in order to obtain the needed interpolation formulae. Each reported diameter was determined along well-defined *x* and *y* axes. The averages of these two measurements, when divided by two, give the radii shown in Table 1. In Section III, we discuss how well these average radii represent the radii of the corresponding least squares circles (LSCs) as determined from circularity measurements.

z / mm	*r* / mm	*R* / mm
40	24.983900	24.984534
35	24.983928	24.984523
20	24.983938	24.984488
5	24.983948	24.984630
0	24.983875	24.984678

Table 1. Average values of *r* and *R* as a function of *z*, along the 40 mm engagement length. The top of the engagement length is at $z = 0$. Values in red are estimated by linear extrapolation of the two previous points [4].

Examples of fitting the data by regression are shown in Figures 1-4. For our limited data set, it was decided that interpolation by regression was preferable to the use of splines.
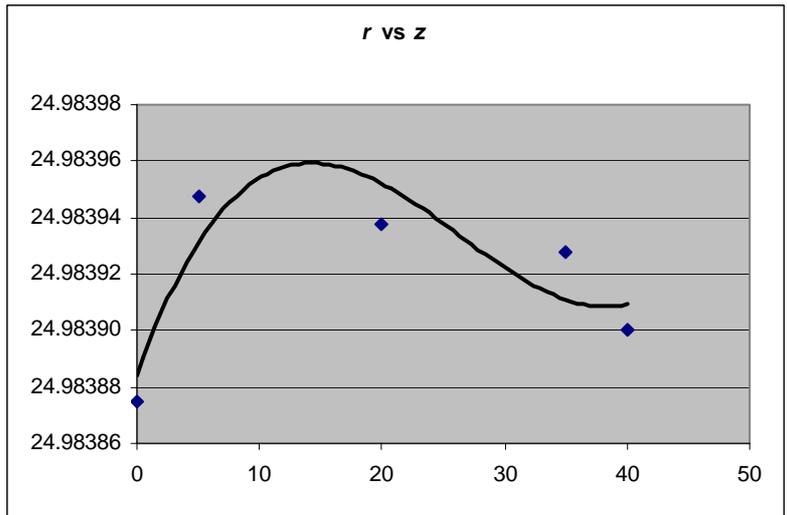
Figure 1. Third-order fit to r/mm as a function of z/mm
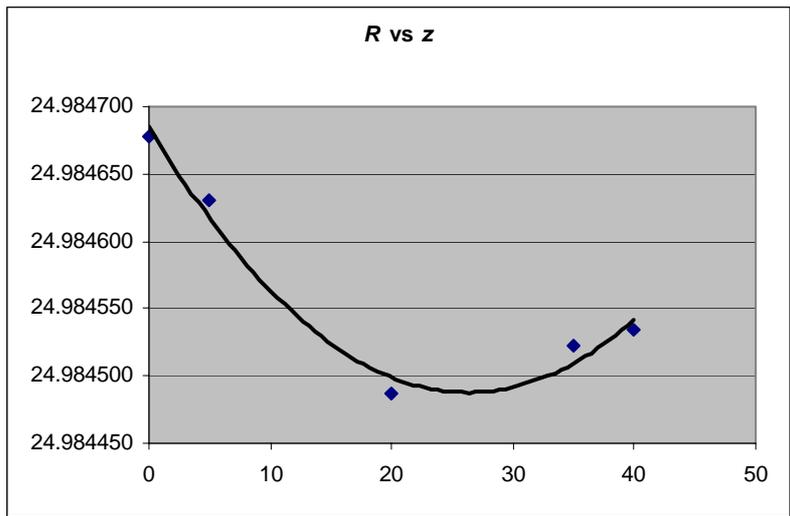
Figure 2. Second-order fit to R/mm as a function of z/mm
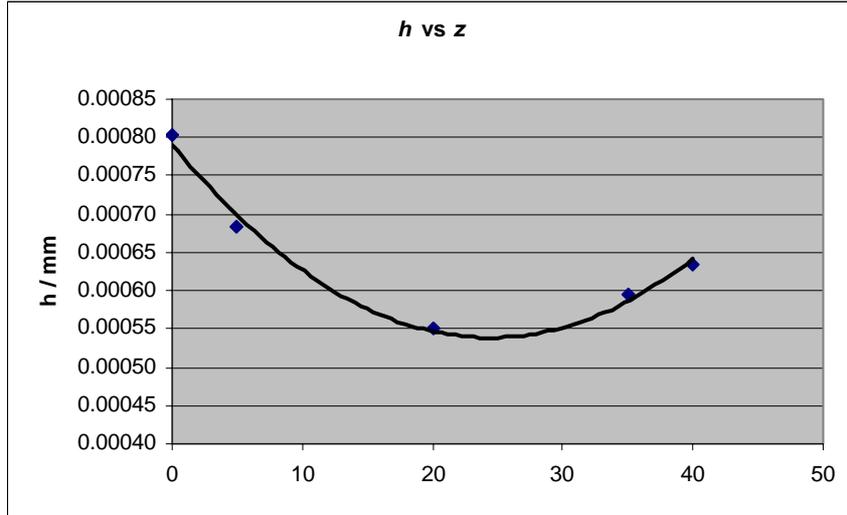
Figure 3. Second-order fit to h/mm as a function of z/mm.
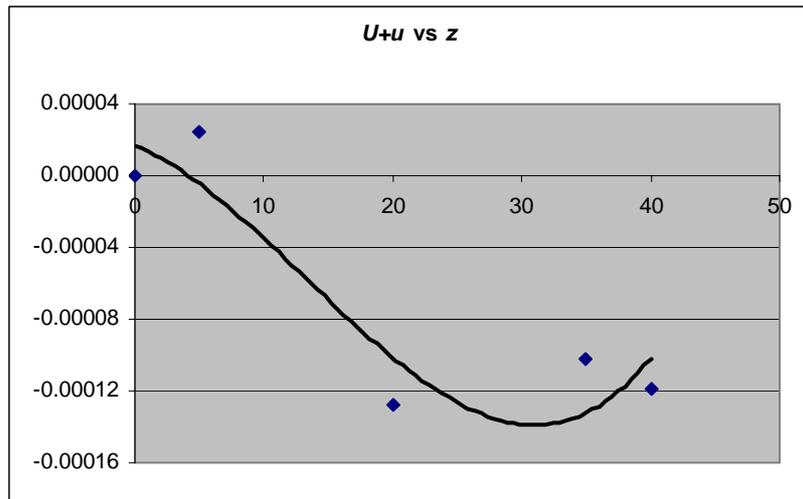
Figure 4. Third-order fit to $(U + u)$/mm as a function of z/mm.

As will be discussed below and in Section III, the results for A are reasonably insensitive to the analytical form of the fit. For example, using only the interpolation curves shown in Figures 1 and 2, we arrive at

$$A_{0,1} = 1961.018\ 411\ \text{mm}^2,$$

while, using r_0 and R_0 from Table 1 and the analytical forms of h and $U+u$ shown in Figures 3 and 4, we arrive at

$$A_{0,2} = 1961.018\ 060\ \text{mm}^2,$$

which is a relative difference in area of 0.2×10^{-6}.

One might be suspicious of the first point in Figure 1. If one eliminates this point and fits the remaining points to a straight line (which of course extrapolates to a very different value of $r(z=0)$), the relative change in $A_{0,1}$ is only 0.11×10^{-6}.

Finally, we mention that one participant in Project 740 [4] derived the effective area by averaging all radial data for the piston and cylinder. Although a conclusion of [4] is that this method gives results that are slightly different to those of the others used by participants, we have used the averaging method for completeness; but we have modified it to take account of our limited data set. Using the curves shown in Figs. 1 and 2, we have estimated the average radius by integrating the argument $(R(z) + r(z))/(2L)$ over the engagement length , $0 < z < L$. The result is

$$A_{0,3} = 1961.019\ 161\ \text{mm}^2,$$

which is in rather good agreement with the more complete analysis. This method is discussed in more detail in Appendix A.

II. Calculation of effective area for operation in the absolute mode, $P(L) = 0$; $P(0) = P_0$

The calculations carried out in Section I are a useful start. We will return to them in Section III in order to analyze a number of uncertainty components. However, we must now calculate A_P, which takes account of nitrogen gas flowing in the gap of the piston-cylinder when the measured pressure is of order P_0 and $P(L)$ is vacuum—the so-called "absolute mode" of operation [1]. Note that the we are *not* calculating the small effect due to the elastic distortion of the piston when it is subjected to a gradient of 1000 hPa across its ends. This effect is treated as an additional coefficient which is supplied by the manufacturer. We assume, however, that correlations between P and h can be neglected in the range $0 < P \leq 1000$ hPa.

Although a formula which is said to apply to the absolute mode is derived in [1], Sutton [2,3] has pointed out that the derivation has not taken into account the fact that the gas flow in the gap begins in the viscous regime at $z = 0$ but ends in the molecular regime. The transition occurs when the Knudsen number is near unity [3,5], in which case the mean free path of the gas flowing in the gap between the piston and cylinder becomes comparable to the separation distance, h.

Following Sutton's derivation, we note that (1) is a special case of a more general formula which, for operation in the absolute mode, may be written as [1,3]

$$A_P = \pi r_0^2 \left\{ 1 + \frac{h_0}{r_0} - \frac{2}{r_0 P_0} \int_0^L I\, dz \right\} \tag{2}$$

where

$$I = (u + wh - w_0 h_0)\frac{dP}{dz} \quad . \tag{3}$$

In [1], w and w_0 are identically equal to ½, reflecting the fact that the neutral surface of a piston-cylinder operating under viscous flow is exactly at $r + h/2$. In Sutton's development [2], w_0 is ½ but w becomes less than ½ as the gas passes through the viscous/molecular transition and the neutral surface moves closer to the piston. For the dimensions of our piston-cylinder, the predicted effect is very small [2] and so we have set $w = ½$. In so doing, the expression within the parentheses in (3) becomes $(u+U)/2$ and thus (2) reduces to equation (23) of [1]. [This is the same as equation (25) of [1], derived for the type I(B) piston-cylinder, after an integration by parts.] To understand why the effect is so small under our conditions of operation, we can take the example of a perfect piston-cylinder with $h = 0.000\,8$ mm. As a worst case, we assume that w takes its zero-pressure value at all pressures along engagement length so that the last term within the parentheses of (2) becomes

$$\frac{1-2w}{r}h\,,$$

which is preceded by a minus sign.

From [2], we estimate $0.500 > w > 0.495$ and thus the relative correction for molecular flow must be considerably less than 0.3×10^{-6} in magnitude.

The pressure gradient in the vertical direction may be determined from the formula

$$P = P_0 - P_0 \left(\int_0^z F^{-1} dz \right) / \left(\int_0^L F^{-1} dz \right), \tag{4}$$

where F is the flow conductance, for which a formula is given in [3] in terms of h and the inverse Knudsen number, f. The latter is itself a function of P and h. f becomes smaller than unity when the mean free path of the gas molecules (nitrogen in our case) becomes greater than h, the separation between the cylinder and piston. The inverse Knudsen number may be expressed as

$$f = hP/c_g. \tag{5}$$

With h in mm and P in Pa, $c_g = 6.5$ Pa mm for nitrogen at 20 °C [6].

Equation (4) must be solved iteratively because F is itself a function of P. After several such iterations, the solution converges to the pressure profile shown in Figure 5. The convergence does not depend strongly on initial conditions. For example, the solution shown in Figure 5 will be reached if the initial condition is $P = P_0$ for $0 \le z \le L$.
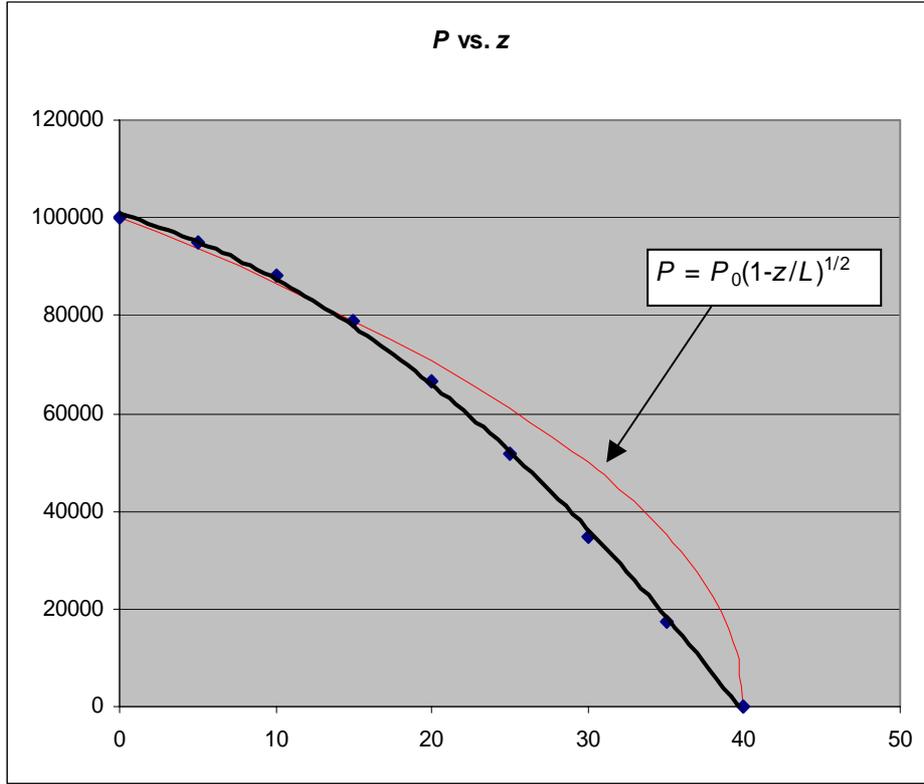
Figure 5. In black, second-order fit to P / Pa as a function of z /mm, as determined by (4).

From (5), the Knudsen number becomes equal to unity at approximately $P = 10$ kPa.

The result of this calculation is

$$A_{P,1} = 1961.017\ 426\ \text{mm}^2.$$

If we had simply assumed that the gas pressure follows the relation $P = P_0(1 − z/L)^{1/2}$ [2][1], this result would have been increased by $0.2 \times 10^{-6}\ A_{P,1}$.

By contrast, Eq. (37) of [1], derived for viscous flow throughout the engagement length, gives

$$A_{P,2} = 1961.015\ 799\ \text{mm}^2$$

(but see discussion in III.E). The relative differences of $A_{0,1}$, $A_{0,2}$, $A_{0,3}$ and $A_{P,2}$ with respect to $A_{P,1}$ are 0.50×10^{-6}, 0.03×10^{-6}, 0.88×10^{-6} and -0.83×10^{-6}, respectively.

We will take $A_{P,1}$ as the effective area of our piston-cylinder.

III. Uncertainty

The uncertainty of $A_{P,1}$ has a number of components that must be considered: A) non-circularity of the piston-cylinder, B) uncertainty of the calibrated diameters, C) sensitivity of the result to engagement length, D) inadequacies of the interpolation formulae used for

---

[1] This is a special case of eq. (32) of Dadson et al. [1], when $h(z)$ is constant over the engagement length.

numerical integration, E) inadequacy of the formulae themselves. For all but E), it is convenient to propagate uncertainties through (1). Note that the integration terms (the third terms within the parentheses of (1) and (2)) introduce only small relative corrections, about 4×10^{-6} in magnitude, to the effective area.

A. Non-circularity

Non-circularity of the piston-cylinder may have introduced a bias error into our estimates of the average radii. Specifically, we introduce an error when the average of the two orthogonal diameters measured for each cross-section does not equal the diameter of the least-squares circle (LSC) determined from circularity measurements [3]. For the calculations discussed here, the worst case occurs at the vacuum end, $z = 40$ mm, for both the piston and the cylinder. The bias errors on the average radius are -20 nm and + 8 nm respectively, although this is consistent with the uncertainty of the calculation (see Section III.B). The starting data were nevertheless adjusted to eliminate the calculated biases of the points and the interpolation curves for $r(z)$ and $R(z)$ were recalculated. The relative change in effective area was less than 0.1×10^{-6}.

The circularity data (which do not constitute a calibration by the LNE) should be consistent with the difference in diameters that were measured along the x and y axes. If Δ_i is the difference in diameters as determined from the circularity chart of the ith section and δ_i is the corresponding estimate based on direct measurement of the two diameters, then the standard deviation of the six $(\Delta - \delta)_i$ is 62 nm. The mean is +20 nm, with 25 nm standard deviation. Therefore, there is no statistical bias between these two methods of determining the diameter difference. However, we suspect that the two diameter measurements are highly correlated. Therefore, it is difficult to explain the large standard deviation observed in the difference of differences. We add a component of $(62 \text{ nm}/2^{1/2})/r_0$ $(u_r 1.8 \times 10^{-6})$ to take account of possible circularity errors.

B. Calibration uncertainty of dimensional metrology

The LNE calibration certificate states that the expanded uncertainty (k=2) of each reported diameter measurement is 0.08 μm. We assume that the diameters measured at two orthogonal diameters are highly correlated so that the average value of r and the average value of R measured for each cross section each have standard uncertainties $u(r)$ and $u(R)$ (k=1) of 0.02 μm. Furthermore, we also assume perfect correlation between measurements of r and R.

It is then possible to carry out an uncertainty analysis using the LNE formulae given in [4]. The result, expressed as a relative standard uncertainty, is virtually identical to that obtained from the simple formula

$$u_r = \frac{u(r) + u(R)}{r_0} \quad , \tag{6}$$

from which $u_r = 1.6 \times 10^{-6}$.

C. Changes in the engagement length

The effective area was recalculated for an engagement length of 36 mm instead of 40 mm and the resulting change is negligible.

The effective area was recalculated for an engagement length of 40 mm but where centre of the cylinder is displaced from $z = 20$ mm to $z = 16$ mm, the centre of the piston remaining at $z = 20$ mm. Again, the resulting change is negligible.

D. Interpolation formulae used for numerical integrations

It is difficult to assess this component of the uncertainty. At the end of Section I, we have already remarked that the interpolation formula for h can be changed from 3rd order in z to linear in z (also eliminating the datum at $z = 0$) with negligible effect. We have also fit a quadratic curve to the $U+u$ data shown in Fig. 4 and this changes results by about 0.2×10^{-6}.

It is clear that the interpolation formulae are not perfect. This is seen from the difference in the calculation results $A_{0,1}$ and $A_{0,2}$. The formulas used to obtain these two results can easily be shown to be mathematically identical. Any discrepancy must be due to the fact that $A_{0,1}$ is obtained using interpolation formulae for r and R, whereas $A_{0,2}$ uses interpolation formulae for $(U+u)$ and h, along with the dimensional measurements for r_0 and h_0.

In addition, we have <u>extrapolated</u> the R data to obtain input values for the extremes of the engagement length. Due to the small number of calibration points along the engagement length, we think it prudent to add a component equal to the LNE calibration uncertainties of the data that we have, in order to allow for all interpolation (and extrapolation) effects. This amounts to $u_r = 1.6 \times 10^{-6}$.

E. The formula

Sutton has estimated that his formula for F propagated a component of relative standard uncertainty of 0.8×10^{-6} in the effective area [3] (note that all uncertainties given in [3] are 99% confidence limits, which we interpret as $k = 3$). It is difficult to assess the uncertainty for our own application, where the molecular flow region is confined to a relatively small fraction of the total engagement length.

As noted above, $A_{P,2}$ differs from $A_{P,1}$ by approximately 0.8×10^{-6}. To see how robust is this difference, we recalculated $A_{P,2}$ after an integration by parts. The integral in question is [1]

$$\int_0^L \frac{d(U+u)}{dz} \left\{ 1 - \frac{\int_0^z \frac{1}{h^3} dx}{\int_0^L \frac{1}{h^3} dx} \right\}^{\frac{1}{2}} dz \qquad (7)$$

and the expression in curly brackets is $P(z)/P_0$. Before integrating (7) by parts, we calculated the power series representation of $(U+u)$ in order to add the constraint $(U(0)+u(0)) = 0$. The integration by parts gives the same result for the integral to 0.01% (0.001×10^{-6} difference in

A). Integrations were carried out using the Romberg method. However, we remarked the following: while the value of $A_{P,1}$ changed by less than 0.05×10^{-6} with the new fit to $(U+u)$, the value of $A_{P,2}$ increased by 0.65×10^{-6}, effectively removing the small discrepancy that had been noted at the end of Section II.

A pertinent article by Delajoud et al. [7] discusses the calibration of a three 50 mm diameter piston-cylinders manufactured by DHI but made of a ceramic material (our piston-cylinder No. 517 is made of tungsten carbide). Three different methods are reported in [7] to calculate the effective area of each piston-cylinder set, all relying on the same dimensional measurements carried out at the NIST. These methods are: simple averaging (as we used to calculate $A_{0,3}$); (1) or its mathematical equivalent (as we used to calculate $A_{0,1}$ and $A_{0,2}$); and Eq. (37) of Dadson et al. [1] (as we used to calculate $A_{P,2}$). For all three piston-cylinders studied in [7], the most serious relative discrepancies are about 1×10^{-6}. Note, however, that their results are tabulated to a relative precision of 0.5×10^{-6}. In any case, our most serious discrepancy among these methods is about 1.7×10^{-6} (between $A_{0,3}$ and $A_{P,2}$). The three piston-cylinders were also calibrated in the gauge mode by cross floating against two different reference gauges traceable to NIST primary standards. Discrepancies for all six measurements with respect to the dimensional calculations ranged from -7×10^{-6} to $+5 \times 10^{-6}$, with three of three of the six results agreeing to within 2×10^{-6}. We do not taken account of these discrepancies in our own uncertainty budget.

To conclude this section, it seems to us prudent to assign a relative uncertainty of 1.5×10^{-6} (type B) to the method used to obtain $A_{P,1}$.

F. Final uncertainty budget

The final budget for the relative standard uncertainty of the effective piston area is given in Table 2 for $A_{P,1} = 1961.017\ 426$ mm^2. Due to the reliance on calibration data and Type B estimates, the number of degrees of freedom is much greater than 10 and need not be calculated in detail.

Component or effect	Standard uncertainty	Sensitivity factor for calculating relative standard uncertainty	Relative standard uncertainty / 10^{-6}
r	20 nm	$1/r$	0.8
R	20 nm	$1/r$	0.8
circularity			1.8
engagement length			<0.1
interpolation			1.6
formula			1.5
total			**3.3**

Table 2. Final uncertainty budget for $A_{P,1}$. Components are considered to be uncorrelated with the exception of *r* and *R*, which are assumed to be perfectly correlated.

The analyses presented in [4] include the uncertainty of r_0, which appears explicitly in (1). It can be shown that the sensitivity factor for r_0 is h_0/r^2 [4]. This is so small compared to $1/r$ that consideration of $u(r_0)$ in our uncertainty budget is not needed.

IV. References

1. Dadson R.S., Lewis S.L., Peggs G.N., *The Pressure Balance (Theory and Practice)*, London, Her Majesty's Stationery Office, 1982, 290 p.

2. Sutton, C.M., *J. Phys. E*, 1980, **13**, 857-859.

3. Sutton, C.M., *Metrologia*, 1993/94, **30**, 591-594.

4. Molinar G., Bergoglio M., Sabuga W., Otal P., Kocas I., Verbeek J., Farar P., *Final Report of EUROMET Project 740*, 2005.

5. Schmidt J.W., Welch B.E., Ehrlich C.D., *Meas. Sci. Technol.*, 1993, **4**, 26-34.

6. O'Hanlon J.F., *A User's Guide to Vacuum Technology*, New York, Wiley, 1980, 402 p.

7. Delajoud P., Girard M., Ehrlich C.D., *Metrologia*, 1999, **36**, 521-524.

8. Schmidt J.W., Yuequin C., Driver R.G., Bowers W.J., Houck J.C., Tison S.A., Ehrlich C.D., *Metrologia*, 1999, **36**, 525-529.

Appendix A

Comparing the technique of averaging radii with other methods

In [4], it is concluded that the technique of averaging radial measurements of the piston and cylinder in order to arrive at an average radius gives results that are slightly different to those of the other methods studied. By contrast, the authors of [7] imply that the technique of averaging radial measurements is a) as successful as other, more complicated methods and b) that this technique gives a result that can be used for cases when P_0 is close to the reference pressure and also when the difference in pressure is about one atmosphere. The explicit equation for averaging radii is given in [8].

Unfortunately, in none of these references is there any indication of how the method of simple averages compares <u>analytically</u> with other methods. In fact, such a comparison is relatively straightforward under reasonable assumptions. We present it here.

i. Method of averages

From [8], the formula for the effective radius, r_e, of the piston-cylinder may be inferred to be

$$r_e^2 = \frac{1}{2}\left(\langle R \rangle^2 + \langle r \rangle^2\right), \tag{A.1}$$

where $\langle R \rangle$ and $\langle r \rangle$ are the respective averages of the cylinder and piston data.

In the following, we will assume the existence of interpolation curves for $R(z)$ and $r(z)$ as described in Section I (see Figs. 1 and 2) so that the averages shown in (A.1) may be found by integration. One may then show that

$$r_e^2 = \left(\frac{1}{2L} \int_0^L (R(z) + r(z))dz \right)^2 \tag{A.2}$$

is the same as (A.1) to first order in h_0/r_0 if the set of (R, r) data is sufficiently dense.

By making use of the identity

$$R(z) + r(z) = R_0 + r_0 + U(z) + u(z), \tag{A.3}$$

the effective area becomes

$$A_e = \pi r_e^2 = \pi r_0^2 \left(1 + \frac{h_0}{r_0} + \frac{1}{r_0 L} \int_0^L (U(z) + u(z))dz \right), \tag{A.3}$$

again to first order in h_0/r_0.

ii. Comparison with other methods

One sees by inspection that (A.3) is identical to (1) under the condition that $h(z) = h_0$, which implies that changes in R and r as a function of z are perfectly correlated.

We now consider under what conditions (A.3) will equal (2), with $w(z) = \frac{1}{2}$. Equality would be achieved if

$$\frac{dP}{dz} = -\frac{P_0}{L} \tag{A.4}$$

and this may in many cases be a reasonable enough approximation to the black curve in Fig. 5. When we recalculate (2) with a linear pressure dependence, given by (A.4), we indeed recover $A_{0,3}$ to within 0.11×10^{-6}.

We conclude that (A.3), and its approximation based on discrete data, can give good agreement when compared to more elaborate schemes [4,7,8] under certain conditions.